May 17th, 4:00 PM

Multiphase Numerical Modelling of Hydraulic Structures With Rapidly Rotating Flows: Stormwater Vortex Hydrodynamic Separator

Sean Mulligan
National University of Ireland Galway, Ireland, sean.mulligan@nuigalway.ie

Dermot McDermott
National University of Ireland, Galway, dermot.mcdermott@nuigalway.ie

Eoghan Clifford
National University of Ireland, Galway, eoghan.clifford@nuigalway.ie

Recommended Citation

Mulligan, Sean (2018). Multiphase Numerical Modelling of Hydraulic Structures With Rapidly Rotating Flows: Stormwater Vortex Hydrodynamic Separator. Daniel Bung, Blake Tullis, 7th IAHR International Symposium on Hydraulic Structures, Aachen, Germany, 15-18 May. doi: 10.15142/T3706S (978-0-692-13277-7).

ISBN 978-0-692-13277-7 DOI: 10.15142/T3706S

Multiphase Numerical Modelling of Hydraulic Structures with Rapidly Rotating Flows: Stormwater Vortex Hydrodynamic Separator

S. Mulligan[1], D. McDermott[1] & E. Clifford[1, 2]
[1]*College of Engineering and Informatics, National University of Ireland Galway (NUIG), Galway, Ireland*
[2]*Ryan Institute, NUI Galway*
E-mail: sean.mulligan@nuigalway.ie

Abstract: *Hydraulic structures exhibiting strongly rotating flows are widely applied in the field of urban and wastewater hydraulics. Given demographic, urban development and climate change challenge, such infrastructure will require significant design innovation. Computational fluid dynamics (CFD) is increasingly an effective and widely used tool to evaluate and optimise new designs and determine performance efficiency for such structures. In this study, a full-scale prototype of a hydrodynamic vortex grit interceptor for stormwater conveyance systems (the BMS Stormbreaker Defender) was investigated using experimental and numerical methods. The prototype was evaluated physically in a full-scale test rig permitting flows of up to 30 l/s. Three-dimensional velocity distributions were obtained along radial profiles using acoustic Doppler velocimetry (ADV). The three-dimensional flow field in the chamber was also modelled using the ANSYS CFX software with a multiphase homogeneous Eulerian-Eulerian approach. In particular, the effectiveness of two-phase flow modelling using the shear stress transport (SST) model with curvature correction was analysed. Good qualitative and quantitative agreements were found between the numerical solutions and the experimental data sets for the four flow scenarios investigated. The results of the CFD evaluation/validation, the practicality of obtained data, and the implications for the design of such a structure are discussed.*

Keywords: *Air-water interface interactions, hydraulic structure design and management, rotating and swirling flows, sewer hydraulics, vortex dynamics, particle separation.*

1. Introduction

Hydraulic structures exhibiting strongly rotating flows are common in the field of hydraulic engineering. Such systems include energy dissipation vortex drop shafts (Hager, 1985; Mulligan, et al., 2016), flow attenuation/regulation chambers (Ackers and Crump, 1960), vortex hydroelectric power applications (Dhakal et al., 2015), strongly curved open channels (Dean, 1928), and hydrodynamic grit settlement chambers (Fenner and Tyack, 1999). With increases in best management practice in stormwater conveyance systems, there has been increased focus on deploying hydrodynamic grit separation systems (Fenner and Tyack, 1997) to intercept particle and debris laden stormwater flows. For example, thousands of hydrodynamic separators have been installed in North America in recent years (Pathapati and Sansalone, 2009). Computational fluid dynamics (CFD) has become an increasingly practical and accurate method to evaluate the performance of stormwater hydraulic structures and to understand flow patterns, pollutant mixing and sediment transport behaviour. Overviews of the opportunities for the use of CFD in urban drainage related applications are presented by Ta (1999), Faram and Harwood (2000) and Harwood (2006), and these further verify the compatibility and merits of CFD application for urban drainage system design and analysis. In the context of hydrodynamic grit separators, CFD has been used increasingly for system optimization and flow pattern analysis (Andoh, 2005).

However, CFD based predictions are highly sensitive to a range of set-up parameters including temporal and spatial discretization, turbulence modelling and approaches to multiphase modelling. In particular, flows exhibiting strong rotation and/or curved free-surfaces can be highly challenging to model using conventional CFD practices due to the presence of strong streamline curvature and highly anisotropic turbulent conditions (Shur et al., 2000, Škerlavaj, 2014; Mulligan, 2015). That said, previous CFD studies on hydraulic structures exhibiting strong rotation have continued to use standard approaches to modelling. For example, a number of studies (Dhakal et al., 2015; Li et al., 2004; Škerlavaj, 2014) tended not to consider interphase capture of the free-surface through the use of a 'fixed-lid' approach. Thus, numerical accuracy is often traded for reduced computational expense (faster simulation run times). As stated by Jarman et al. (2008), '*prediction of water surface profiles, while seemingly fundamental, is actually absent from the majority of studies*.' In addition, previous studies (Tokyay and Constantinescu, 2005; Suerich-Gulick et al., 2006; Stephens and Mohanarangam, 2010) suggest that numerical modelling of curving flows is strongly dependent on the type of turbulence model employed. Despite such findings, there are a number of recent CFD studies on rotating flow structures and hydrodynamic grit separators that have not fully considered the choice of turbulence model (Dhakal et al., 2015, Tyack and Fenner, 1999; Ying et al., 2012). For example, Ying et al (2012), when studying vortex hydrodynamics separators, assumed that there is isotropy of Reynolds stresses which is generally not the case for such flows. Previous studies have concluded that the eddy viscosity models significantly overestimate the turbulence in areas of strong streamline curvature (Tokyay and Constantinescu, 2005; Suerich-Gulick et al., 2006). Therefore, to account for system rotation and curvature, Spalart and Shur (1997) developed a curvature correction (CC) to the RANS equations. So far, the CC principle has only been tested for a small range of free-surface vortex flow applications (Škerlavaj et al., 2011; Stephens and Mohanarangam, 2010; Škerlavaj et al., 2014; Mulligan, 2015) with no direct studies on the topic of the CC approach in multiphase simulations in vortex separators.

Through a physical-numerical comparison at prototype scale, this study aims to investigate the performance of multiphase CFD modelling including analysing the effect of curvature correction principle of Spalart and Shur (1997). The study is undertaken on the Stormbreaker Defender, (supplied by Butler Maufacturing Services (BMS)) at a scale of 1/1. ANSYS CFX is employed for all three-dimensional multiphase simulations. The results of the CFD evaluation/validation and the practicality of obtained data is discussed subsequently.

2. Case Study: Stormbreaker Defender Hydrodynamics Grit Separator (Prototype ~1/1)

Vortex hydrodynamic separators are generally deployed to remove (i) sediments and (ii) floating material from storm water. However, some systems are also often useful for removing oils and hydrocarbons. In this study, a prototype of the Butler Manufacturing Services (BMS) Stormbreaker Defender vortex hydrodynamic separator (Figure 1(a) and (b)) was investigated. In this system, flow is conveyed to the chamber via an inlet pipe arranged tangentially within the gap between an inner and outer cylinder which induces a vortex flow in the device. A rectangular weir located on the internal cylinder permits flow into the inner chamber where it discharged in an upward direction through the outlet pipe. The Stormbreaker Defender utilises the available flow of the fluid conveyed through a tangential inlet to induce vortex flow. The resulting centrifugal forces push heavier particles outwards radially to the chamber walls where the gravitational forces become more dominant in the boundary layer to enhance separation (Ogawa, 1992).

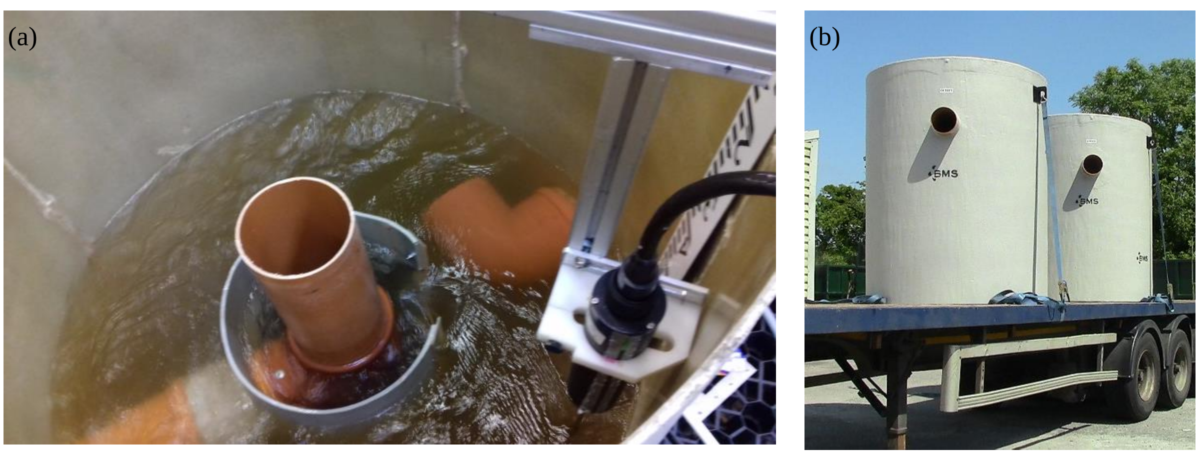

Figure 1: (a) Stormbreaker Defender chamber with Acoustic Doppler Velocimetry (ADV) probe used in this study and (b) Stormbreaker Defender (Model C) (image courtesy of Butler Manufacturing Services http://www.butlerms.com/)).

3. Experimental and Numerical Methodology

3.1. Experimental Analysis

The experimental test rig consisted of a hydraulic flow recirculation loop occupying a floor area of 6 m × 2 m at the NUI Galway Hydraulics and Aerodynamics Laboratory (Figure 2 (a) and (b)). Water was pumped from a storage tank using a centrifugal pump ($Q = 0$ to 30 l/s) into a header tank which controlled the upstream water level/pressure, conveying water inline to the hydrodynamic separator chamber. Flow (and water level) were controlled using a gate valve. Water leaving the hydrodynamic separator chamber passed through an acrylic pipe section to obtain water level readings and observe multiphase flow characteristics. The flow subsequently passed into a flow measurement flume comprising of a 90-degree v-notch weir (USBR, 1997) equipped with a depth gauge to measure the height above the weir (h_{weir}) at a distance of $5h_{weir}$ upstream of the notch.

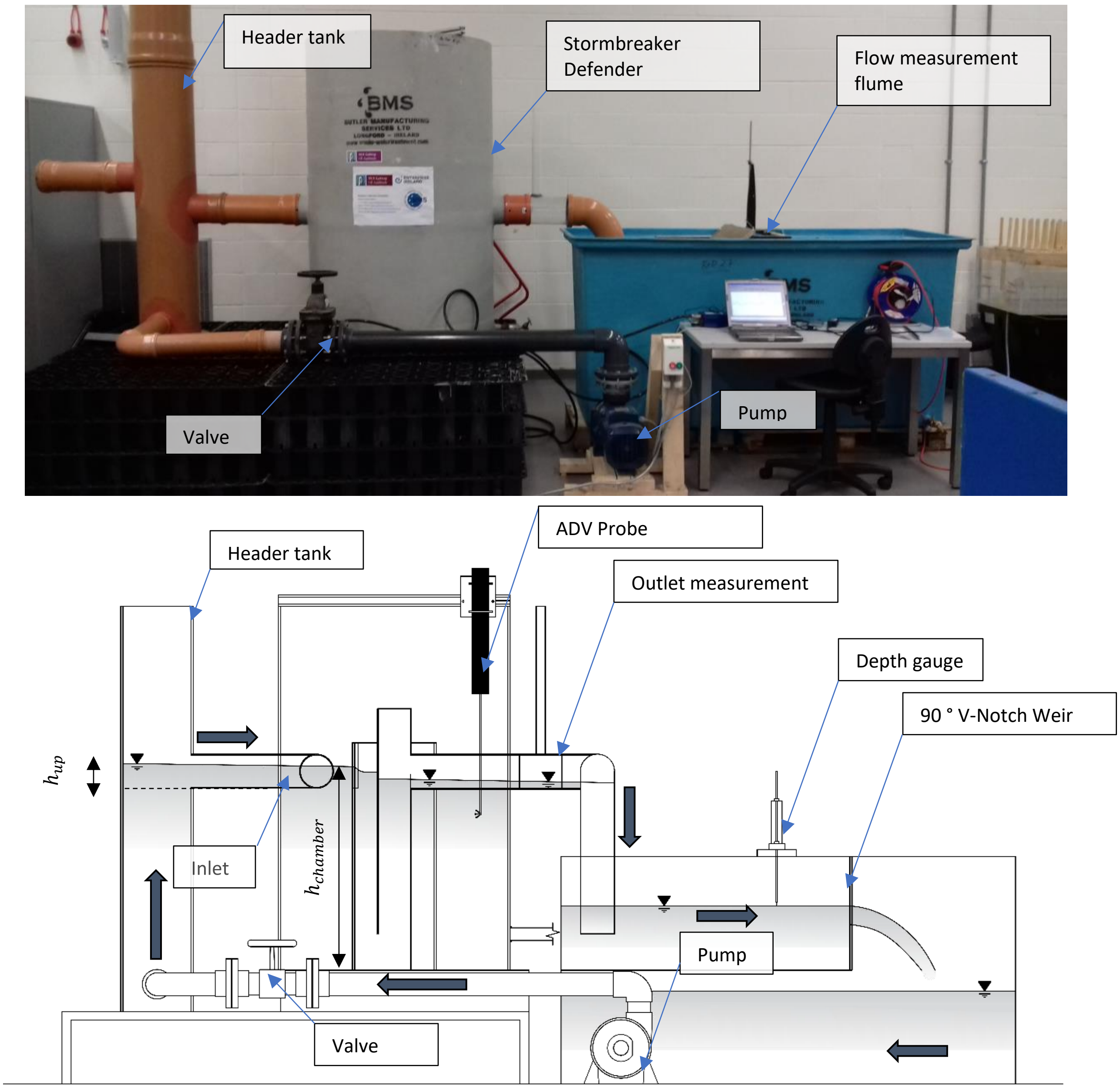

Figure 2: (a) Full scale hydraulic test rig for Stormbreaker Defender and (b) cross sectional schematic of hydraulic test rig for Stormbreaker Defender highlighting the main experimental components.

Water level readings were obtainable in the header tank h_{up} using a manometer, in the vortex chamber $h_{chamber}$ using a staff gauge located at the chamber perimeter, and in the outlet pipe h_{down} using a level gauge enabling the head-losses to be determined throughout the system. During testing, a steady flow was established when the water in the header tank and vortex chamber maintained a constant depth. During low flowrates, l/s$\leq Q \leq$15 l/s, small fluctuations in the chamber water levels resulted in an approximate error of $\pm$ 1 % of the depth reading. However, for higher flows ($Q \geq$ 15 l/s), the fluctuations were found to be in the region of $\pm$ 2 % for $h_{chamber}$ increasing to $\pm$ 5 % for h_{up}.

Velocity measurements were conducted using a Nortek Vectrino 10-MHz acoustic Doppler velocimeter (ADV or NDV). Instantaneous three-dimensional velocity components (x, y, z) along radial profiles in the flow field were obtained using a three-beam, side-looking probe. The probe was suspended on a sliding system installed on an aluminum item bridge system. This permitted horizontal and vertical velocity profiles to be obtained at two radial sections (X and X'), as outlined in Figure 4, which were positioned at a height of 0.5 m above the base of the chamber. For each profile, the velocity was acquired at 30 mm centered along the horizontal datum. Prior to each measurement, the signal-to-noise ratio (SNR) and the correlation were checked for conformance with the recommended values. The velocity range was adjusted to span the entire range of measured velocities determined from flow continuity through the annular flow section (see V_{avg} and V_{in} in Table 1). The control volume for measurement was maintained at 9 mm. Two horizontal profiles (X and X') obtained the tangential velocity v_θ, radial v_r, and axial v_z velocity profiles for the four flow conditions (A, B, C and D) outlined in Table 1. Each 3D velocity reading was obtained for a duration of 30 seconds at 25 Hz (Δt =0.04s) to obtain a 750 point time series.

Table 1: Test cases and hydraulic variables investigated in this study.

Test Case	**Flowrate (l/s)**	$\boldsymbol{h_{chamber1}}$ **(m)**	$\boldsymbol{h_{up}}$ **(m)**	$\boldsymbol{V_{avg}}$ * **(m/s)**	$\boldsymbol{V_{in}}$** **(m/s)**	$\boldsymbol{\Gamma_\infty}$*** **(m/s)**	**Fr**$_{\mathbf{chamber}}$
A	2.021	0.712	0.110	0.008	0.114	0.216	0.007
B	6.900	0.820	0.250	0.024	0.391	0.736	0.020
C	14.273	1.000	0.528	0.041	0.808	1.522	0.034
D	18.655	1.115	0.740	0.048	1.056	1.990	0.039

*Average annulus velocity: $V_{avg} = Q/(Bh_{chamber})$
** Annulus Froude number: $Fr_{chamber} = V_{avg}/\sqrt{gD}$ (D = hydraulic radius of outer cavity)
***Chamber bulk circulation: $\Gamma_\infty = 2\pi V_{in} r_{in}$

3.2. Numerical Analysis

Three-dimensional, multiphase numerical modelling of the vortex flow structure was performed using ANSYS CFX (V14.5) which uses a hybrid FEM/FVM (finite element based/finite volume method) approach to discretise the Navier-Stokes Equations. Previous numerical analyses performed on strong free-surface vortex flows specify best practice guidelines as follows:

- Radially structured or quasi-structured mesh arrangement (Suerich-Gulick et al., 2006; Mulligan et al. 2015).
- Choice of resolution of the numerical scheme has no major effect on the tangential and axial velocity profile (Skerlavaj et al., 2014).
- Transient modelling is necessary to resolve flow instabilities (Mulligan et al. 2015).
- Shear stress transport (SST) with curvature correction (CC) can provide a significant improvement in the solution accuracy (Skerlavaj et al., 2014; Mulligan, 2015).

The boundary condition configuration assigned a mass flow at the inlet and a static pressure condition at the outlet. A zero pressure outlet was provided with the outlet position located 15 times the inlet pipe diameter downstream. The top of the chamber was simulated as an open boundary condition with zero relative pressure. A no slip boundary condition was imposed to the walls of the vessel. The two-phase fluid domain was modelled using a homogeneous Eulerian-Eulerian multiphase flow model. This is a limiting case of the full Eulerian-Eulerian model which assumes that interphase momentum transfer is negligible. This was valid for the current test case where the phases are completely stratified, the interface is well defined, and interphase mixing is minimal. In the homogenous approach, both phases are treated as interpenetrating continua parted by a well-defined interface and share a common velocity, pressure and turbulence field. Therefore, cells that are located away from the interfacial zone will be representative of either air or water, and cells in the vicinity of this zone will contain a mixture of both. As a conservative measure, a high-resolution scheme (second order accurate) was used to model advection and turbulence numerics. Both the standard SST and SST-CC were tested for comparative purposes using Test Case B.

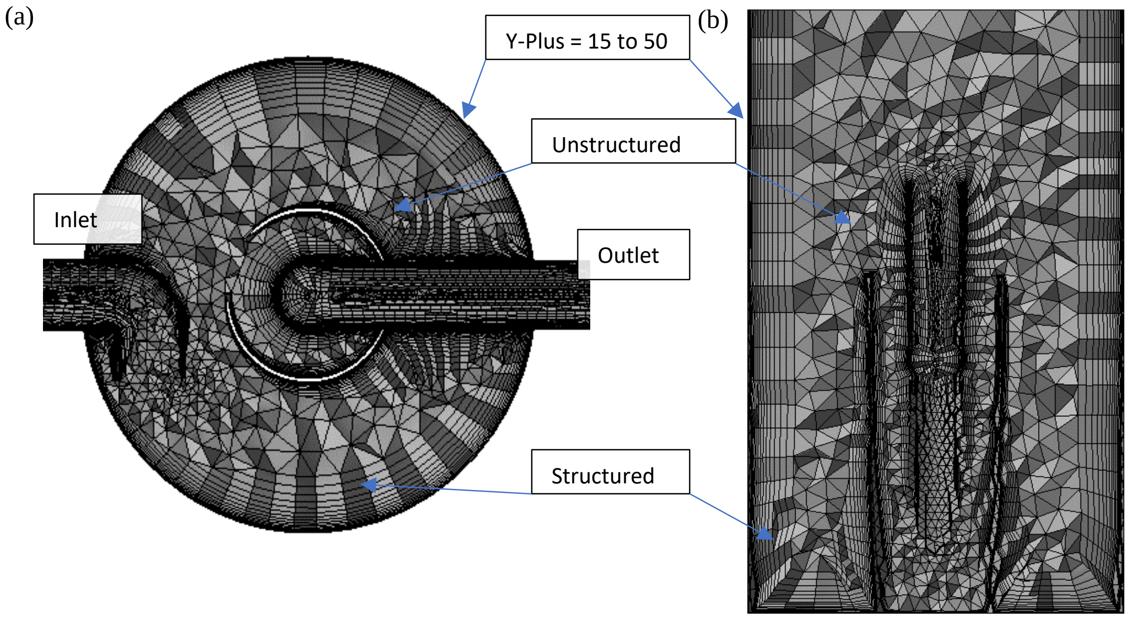

Figure 3: (a) Plan and (b) end view of hybrid (structured/unstructured) meshing arrangement (mesh independent case).

The flow domain was discretised using a quasi-structured radial meshing arrangement as shown in Figures 3 (a) and 3 (b); 3.18 x 10^5 elements were used with a minimum cell size of 5 mm applied in areas where strong gradients were expected. A Y-Plus of 15 to 50 was enforced on all the chamber walls to resolve the boundary layer. Each test case was modelled using a transient simulation for time steps $\Delta t = 0.1$, 0.5, 1.0 s. A conservative physical simulation time of T = 30 seconds was chosen for all physical test cases as per Table 1. The target value of the normalised residual for each flow variable was set to 10^{-5}.

4. Results and Discussion

4.1. Model Sensitivity and General Observations

CFD validation was performed by comparing the water surface, tangential, radial and axial velocities profiles with those obtained from the experiment. The numerical velocity data was obtained along the numerical profile as outlined in Figure 4 (a) which represented an average profile located between Section $X - X$ and Section $X' - X'$. This profile was also located at 0.5 m above the chamber base. Early results (not presented here) indicated that the solution appeared to be independent of time step below $\Delta t = 0.5$. Figure 4 (b) presents the comparison between the standard SST and SST-CC approaches using the tangential velocity profile. In both cases, the general trend (velocity increasing outwards) and magnitude of the tangential velocity profile are predicted well for both the standard and curvature correction approaches. The SST-CC solution has a reduced velocity magnitude closer to the tank perimeter. Based on the available data, it was difficult in this situation to assess whether there was additional merit in adopting the SST-CC for the hydrodynamic separator application. Despite this finding, the SST-CC was adopted with a timestep of 0.1 s for the foregoing analysis.

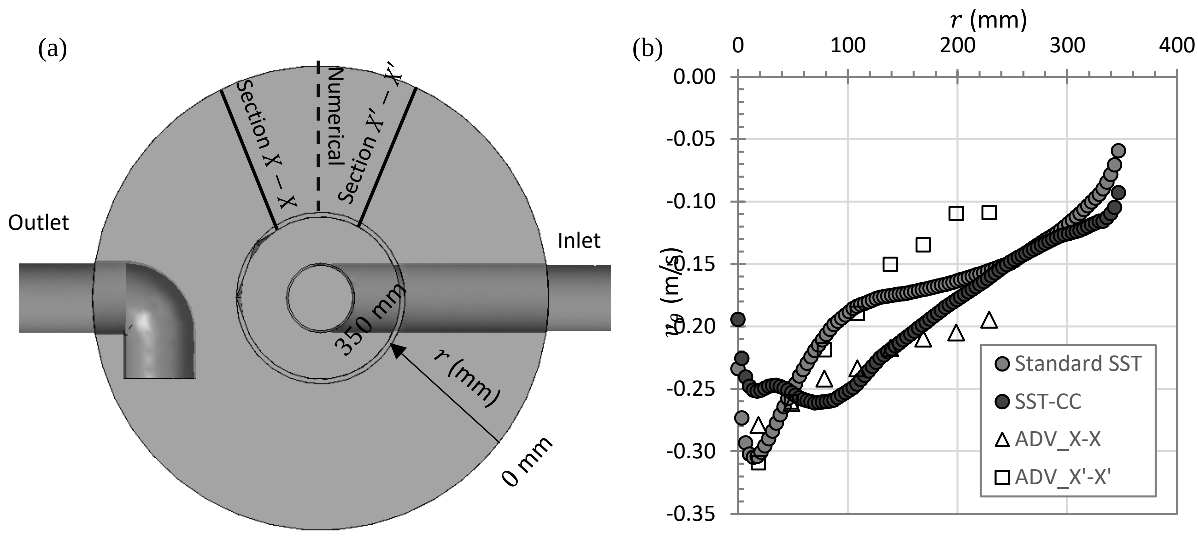

Figure 4: (a) Plan of hydrodynamic separator highlighting the horizontal profiles investigated for ADV and CFD and (b) tangential velocity distribution in the radial direction comparing the Standard SST and SST with Curvature Correction to the ADV data.

4.2. Free-Surface Profiles and Depth Discharge Relationship

Figure 5 (a-d) depicts the predicted water surface profile as an iso-surface (water volume fraction ϕ_w= 0.5) for each of the test cases in Table 1. An good prediction of the water surface position and profile was generated for each case. This agreement was further reinforced by the depth-discharge comparison (shown in Figure 6) for both the chamber depth and upstream depth.

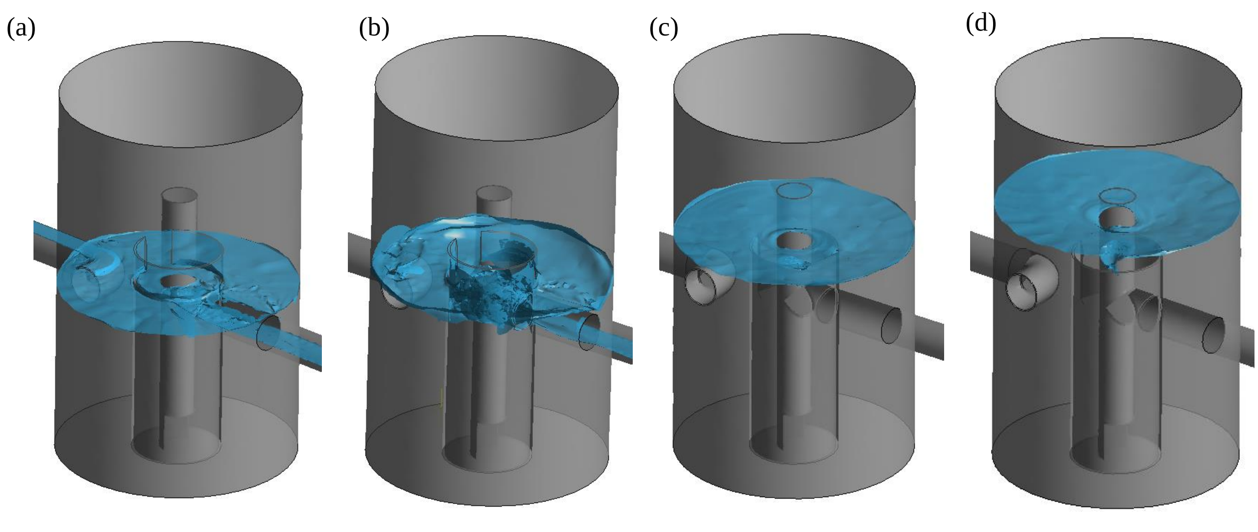

Figure 5: Free-surfaces in the hydrodynamic separator for (a) Q = 2.021 l/s (b) Q = 6.900 l/s, (c) Q =14.273 l/s and (d) 18.655 l/s.

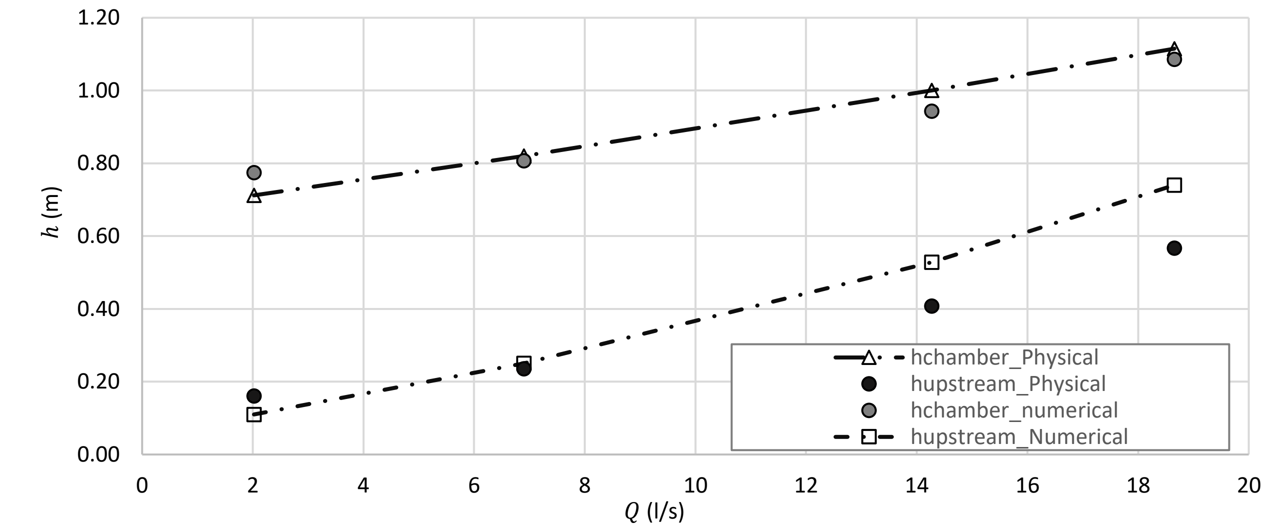

Figure 6: Experimental and numerical comparison for the depth-discharge relationships.

4.3. Tangential Velocity Distributions

A comparison of the tangential velocity distribution for each case is presented in Figure 7 (a-d). The ADV data for Sections $X - X$ and $X' - X'$are presented with error bars representing temporal variation of the velocity over the measurement duration. Larger error bars were entrained for measurements obtained close to the outer wall due to acoustic signal scattering. In general, all profiles (apart from Case A) highlighted a good prediction of the tangential velocity profile.

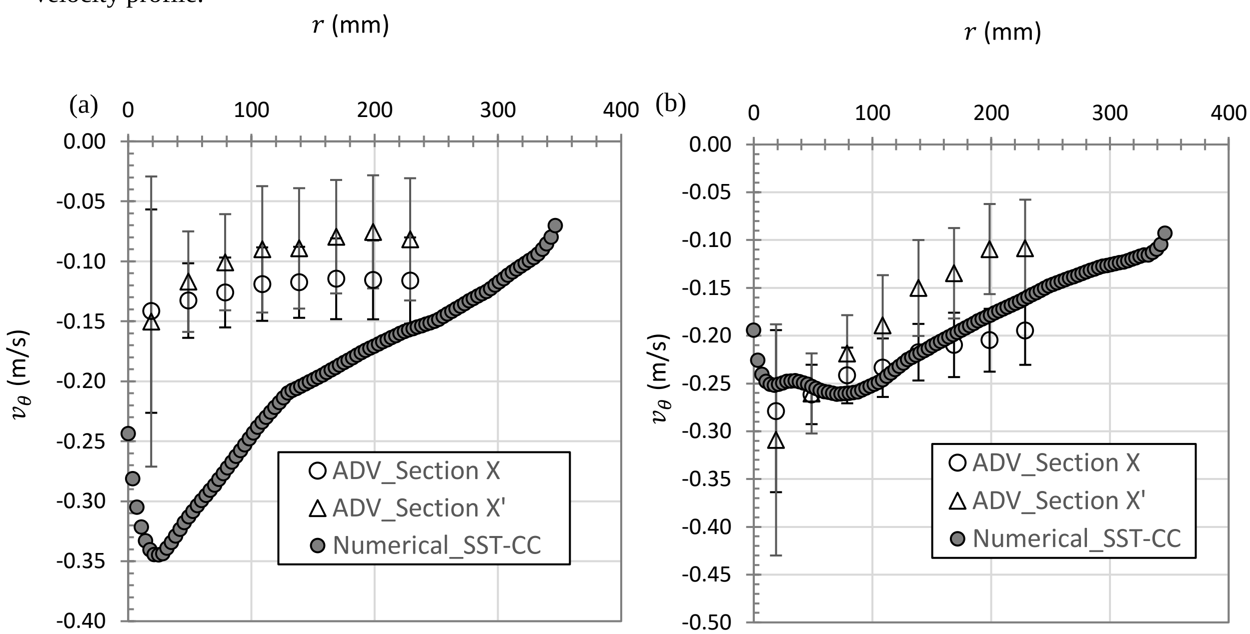

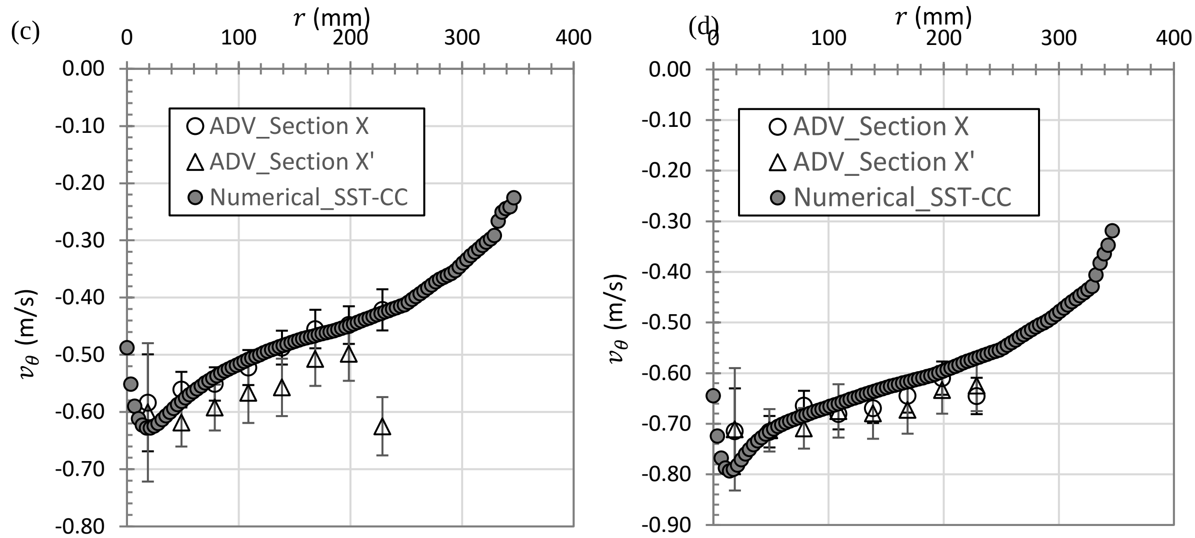

Figure 7: Physical-numerical comparisons of the tangential velocity distributions for (a) Q = 2.021 l/s (b) Q = 6.900 l/s, (c) Q =14.273 l/s and (d) Q =18.655 l/s.

4.4. Axial and Radial Velocity Distributions

As can be seen in Figure 8 (a and b), the comparison of numerical and experimental profiles did not maintain the same level of consistency as the tangential velocity. This was attributed to the steadiness of the primary tangential flow field compared to the secondary axial and radial currents which inherit significant levels of turbulence. This was demonstrated by the large error bars for the ADV datasets showing large variation in the velocity readings. However, in both cases, the numerical profiles fell within the error bars which was considered to be a good prediction.

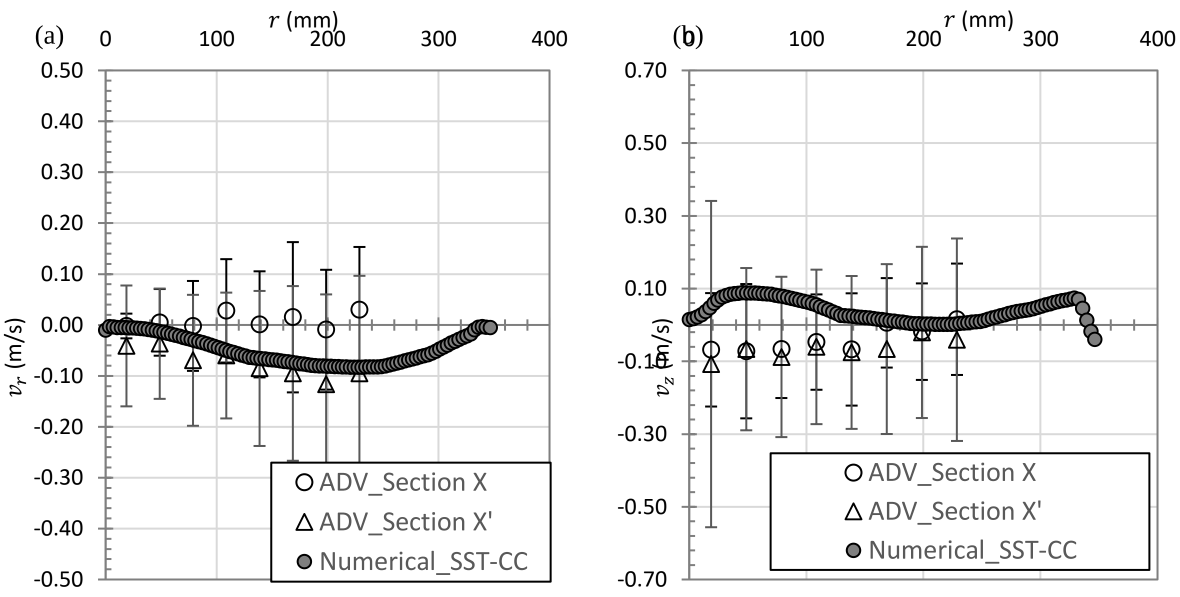

Figure 8: Physical-numerical comparisons of the (a) radial and (b) axial velocity distributions for Q = 6.900 l/s.

4.5. Chamber Hydrodynamics

In general, the previous sections highlighted the value and accuracy of CFD modelling for hydrodynamic separator structures with good predictions made of both the free-surface and tangential velocity profiles. The findings of this study would suggest that CFD has significant merit for application in hydrodynamic separators and perhaps other flows with strong rotational characteristics to assess key performance parameters and significantly enhance and optimize the design process. For example, water velocity streamlines in Figure 9 (a) can be used to qualitatively and quantitatively assess residence times and removal performance. Contours of the velocity in the chamber (Figure 9(b)) can be used to highlight problematic flow phenomena occurring in the chamber. Another issue with hydrodynamic separators is that they tend to scour and resuspend settled material during high flow conditions. Figure 9 (c) highlights likely areas where scour is byusing bed shear stress contours.

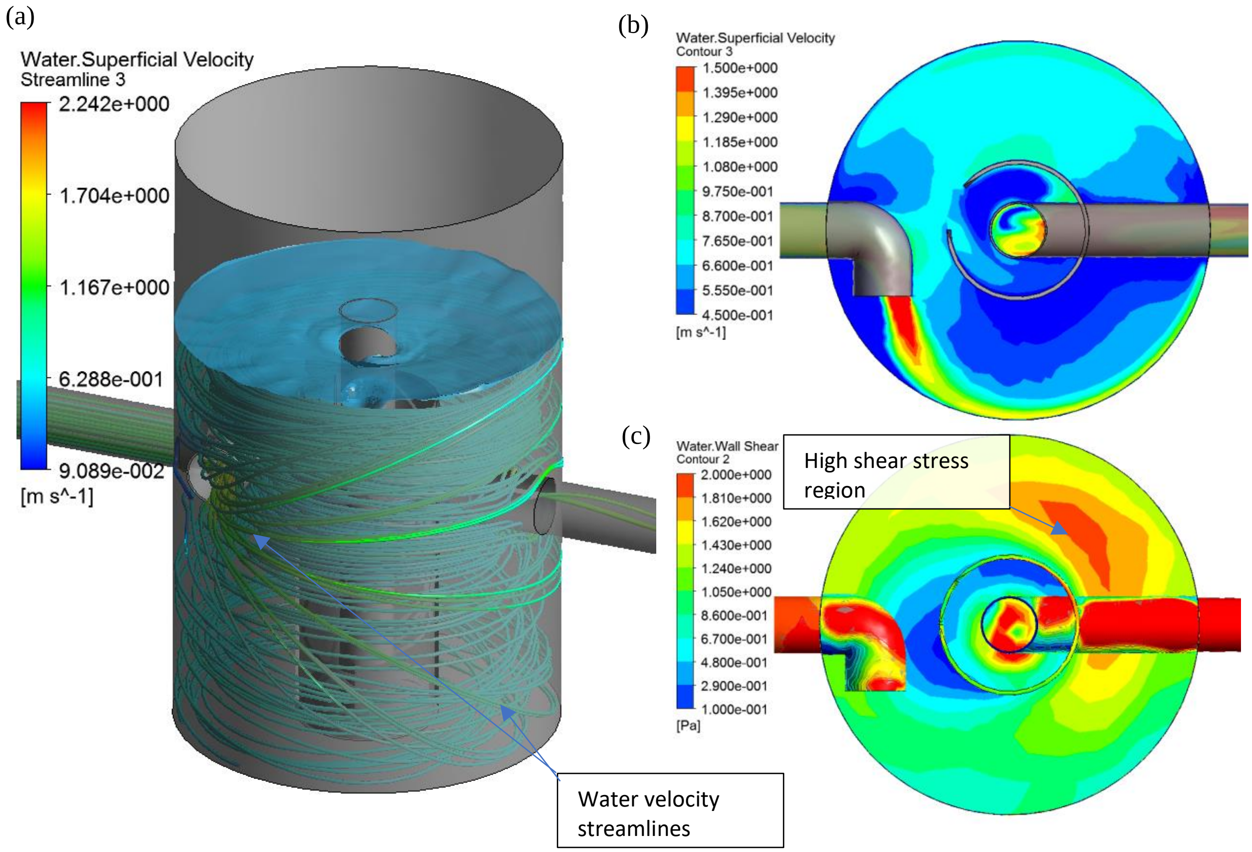

Figure 9: (a) Water velocity streamlines in the Stormbreaker defender, (b) velocity contours highlighting distinguishable flow phenomena and (c) shear stress distribution on the chamber floor highlighting areas susceptible to particle resuspension.

5. Conclusions

As computational hardware and software resources become more advanced, computational fluid dynamics (CFD) is becoming increasingly utilised as part of simulation schemes for hydraulic structures in urban drainage. However, only a limited number of past studies investigating rotating flow hydraulic structures that (i) adopt suitable turbulence and multiphase approaches, particularly in vortex hydrodynamic separators, and (ii) leverage large-scale experimental data have to-date been carried out. This study found that a two phase CFD model with standard approach to turbulence closure can yield valuable results. This was concluded based on good agreements between the experimental and numerical free-surfaces and comprehensive velocity data sets. Following this case study, it can be concluded that CFD is arguably a powerful and accurate tool available for analysing and optimizing rotational flow structures such as the hydrodynamic grit separators. Following some considerations for mesh arrangement and transient modelling, good CFD solutions can be obtained for standard approaches to turbulence modelling. This was demonstrated by good comparisons obtained between the numerical and experimental datasets obtained in a full-scale prototype of the Stormbreaker Defender hydrodynamic separator technology.

6. Acknowledgements

The authors would like to express their gratitude to Butler Manufacturing Services (Longford, Ireland) for making available the Stormbreaker Defender technology prototype and funding the investigation. The authors would also like to acknowledge the funding from Enterprise Ireland (IV-2016-0055-T) and additional support received by NUIG laboratory technical staff.

7. References

Ackers, P. and Crump, E.S., (1960). The Vortex Drop. *Proceedings of the Institution of Civil Engineers*, 16(4), pp.433-442.

Andoh, B., (2005). Computer Simulation Saves in Design of Hydrodynamic Vortex Separator. *Industrial WaterWorld*, *6*(3), pp.18-19.

Dhakal, S., Nakarmi, S., Pun, P., Thapa, A.B. and Bajracharya, T.R., (2014). "Development and testing of runner and conical basin for gravitational water vortex power plant." *Journal of the Institute of Engineering*, 10(1), pp.140-148.

Dean, W.R., (1928), November. Fluid Motion in a Curved Channel. *In Proceedings of the Royal Society of London A: mathematical, physical and engineering sciences* (Vol. 121, No. 787, pp. 402-420). The Royal Society.

Fenner, R.A. and Tyack, J.N., (1997). "Scaling laws for hydrodynamic separators." *Journal of Environmental Engineering*, 123(10), pp.1019-1026.

Faram, M. G. and Harwood, R. (2000). CFD for the water industry; the role of CFD as a tool for the development of wastewater treatment systems. *Fluent Users' Seminar*. Sheffield, UK, Fluent.

Jarman, D.S., Faram, M.G., Butler, D., Tabor, G., Stovin, V.R., Burt, D. and Throp, E., (2008). Computational fluid dynamics as a tool for urban drainage system analysis: A review of applications and best practice.

Li, S., Lai, Y., Weber, L., Silva, J. M. and Patel, V. (2004) "Validation of a three dimensional numerical model for water-pump intakes." *Journal of Hydraulic*.

Mulligan, S., Casserly, J. and Sherlock, R., (2016). Effects of Geometry on Strong Free-Surface Vortices in Subcritical Approach Flows. *Journal of Hydraulic Engineering*, 142(11), p.04016051.

Mulligan, S., (2015). Experimental and numerical analysis of three-dimensional free-surface turbulent vortex flows with strong circulation. PhD Dissertation. Institute of Technology, Sligo.

Ogawa, A., (1992). *Vortex flow*. CRC Press.

Harwood, R. (2006). Computational flow modeling applications expand into the water industry. *Water and Wastewater International* 21(6): 32-34.

Hager W.H. (1985). "Head-discharge relation for vortex shaft" *Journal of Hydraulic Engineering*, 111(6),1015–1020.

Pathapati, S.S. and Sansalone, J.J., (2009). "CFD modeling of a storm-water hydrodynamic separator." *Journal of Environmental Engineering*, 135(4), pp.191-202.

Shur, M. L., Strelets, M. K, Travin, A. K, and Spalart P. R., (2000). "Turbulence modeling in rotating and curved channels: assessing the Spalart-Shur correction," *AIAA Journal*, vol. 38, no. 5, pp. 784–792.

Škerlavaj, A., Škerget, L., Ravnik, J. and Lipej, A. (2014). "Predicting Free-Surface Vortices with Single-Phase Simulations." *Engineering Applications of Computational Fluid Mech*anics, 8(2), pp. 193-210.

Spalart, P.R. and Shur, M., (1997). On the sensitization of turbulence models to rotation and curvature. *Aerospace Science and Technology*, 1(5), pp.297-302.

Stephens, D.W. and Mohanarangam, K., (2010). Turbulence model analysis of flow inside a hydrocyclone. *Progress in Computational Fluid Dynamics, an International Journal*, 10(5-6), pp.366-373.

Suerich-Gulick, F., Gaskin, S., Villeneuve, M., Holder, G. and Parkinson, E., (2006). Experimental and numerical analysis of free surface vortices at a hydropower intake.

Ta, C. T. (1999). Current CFD tool for water and waste water treatment processes. *American Society of Mechanical Engineers, Pressure Vessels and Piping Division* 396: 79-85.

Tokyay, T.E. and Constantinescu, S.G., (2005). Large eddy simulation and reynolds averaged Navier-Stokes simulations of flow in a realistic pump intake: A validation study. In Impacts of global climate change (pp. 1-12).

Tyack, J.N. and Fenner, R.A., (1999). Computational fluid dynamics modelling of velocity profiles within a hydrodynamic separator. *Water science and technology*, 39(9), pp.169-176.

Ying, G., Sansalone, J., Pathapati, S., Garofalo, G., Maglionico, M., Bolognesi, A. and Artina, A., (2012). Stormwater treatment: examples of computational fluid dynamics modeling. *Frontiers of Environmental Science & Engineering*, pp.1-11.